PERGAMON

International Journal of Solids and Structures 39 (2002) 483–497

INTERNATIONAL JOURNAL OF SOLIDS and STRUCTURES

www.elsevier.com/locate/ijsolstr

Overall behavior of two-dimensional periodic composites

Federico J. Sabina [a,*], Julián Bravo-Castillero [a,b], Raúl Guinovart-Díaz [b], Reinaldo Rodríguez-Ramos [b,c], Oscar C. Valdiviezo-Mijangos [a,d]

[a] *Instituto de Investigaciones en Matemáticas Aplicadas y en Sistemas, Universidad Nacional Autónoma de México, Apartado Postal 20-726, Delegación de Alvaro Obregón, 01000 Mexico D.F., Mexico*

[b] *Facultad de Matemática y Computación, Universidad de la Habana, San Lázaro y L, Vedado, Habana 4, CP-10400, Cuba*

[c] *Instituto de Ingeniería, Universidad Nacional Autónoma de México, Apartado Postal 70-472, Delegación Coyoacán, 04510 Mexico D.F., Mexico*

[d] *Posgrado en Ciencias de la Tierra, Instituto de Geofísica, UNAM, Ciudad Universitaria, 04510 Mexico D.F., Mexico*

Received 31 August 2000; in revised form 26 March 2001

Abstract

The overall properties of a binary elastic periodic fiber-reinforced composite are studied here for a cell periodicity of square type. Exact formulae are obtained for the effective stiffnesses, which give closed-form expressions for composites with isotropic components including ones for empty and rigid fibers. The new formulae are simple and relatively easy to compute. Examples show the dependences of the stiffnesses as a function of fiber volume fraction up to the percolation limit. The specific example of glass fibers in epoxy yields new curves, which correct those displayed before by Meguid and Kalamkarov. Comparison with experimental data is very good. Bruno, Hill and Hashin's bounds are compared with the exact solution. In most cases, the latter is very close to a bound in a given interval. A useful fact to know, where the easy formula afforded by the bound is advantageous. Plots of effective properties are also given for values of the shear moduli ratio of the two media. The overall parameters in the cases of empty and rigid fibers are also shown. The exact formulae explicitly display Avellaneda and Schwarts's microstructural parameters, which have a physical meaning, and provide formulae for them. The equations easily lead to Hill's universal relations. © 2001 Elsevier Science Ltd. All rights reserved.

Keywords: Fiber-reinforced composites; Isotropic components; Empty fibers; Rigid fibers; Asymptotic homogenization; Tetragonal symmetry

1. Introduction

Here the concerned problem of finding effective properties is related to materials that have a periodic microstructure. Methods applied to composites with a random distribution of inclusions such as the self-consistent technique can be found in various textbooks (Aboudi, 1991; Christensen, 1991; Nemat-Nasser and Hori, 1999). For periodic media, on the other hand, Fourier series methods have been applied by

* Corresponding author. Tel.: +52-56-223563; fax: +52-56-223564.
E-mail address: fjs@uxmyml.iimas.unam.mx (F.J. Sabina).

0020-7683/01/$ - see front matter © 2001 Elsevier Science Ltd. All rights reserved.
PII: S0020-7683(01)00107-X

Iwakuma and Nemat-Nasser (1983) and more recently by Luciano and Barbero (1994). Also, Aboudi (1991) introduced the so-called method of cells, which covers a wide range of applications. An alternative technique, in the absence of exact or numerical solutions, are the bounding methods, which offer the capability of providing a limited range of possibilities for the relevant property. Thus the bounds of Hashin, Hill, Hashin and Shtrikman (Christensen, 1991), Bruno (1991) and many others (see, for instance, Nemat-Nasser and Hori, 1999). The asymptotic homogenization method (Bensoussan et al., 1978; Sánchez-Palencia, 1980; Lions, 1981; Pobedrya, 1984; Bakhvalov and Panasenko, 1989; Oleinik et al., 1992; Parton and Kudryavtsev, 1993; Kalamkarov and Kolpakov, 1997) is another technique, which can produce closed-form solutions (Pobedrya, 1984; Rodríguez-Ramos et al., 2001) or numerical solutions upon solving the so-called cell problems (see, references in Rodríguez-Ramos et al., 2001). Here the problem of finding the effective properties of a two-phase fiber-reinforced composite is addressed. Elastic isotropic materials are considered and fibers distributed periodically along the x_1- and x_2-directions are studied by means of the asymptotic homogenization method. Exact closed-form formulae are provided directly from the formulation of Rodríguez-Ramos et al. (2001) in a manner which is suitable for a relatively easy computation. The formulae, for the limiting cases of empty and rigid fibers, are also obtained from the original formulae. It must be mentioned that Pobedrya (1984), Parton and Kudryavtsev (1993) and Meguid and Kalamkarov (1994) also applied the asymptotic homogenization method to a fiber-reinforced composite with only isotropic elastic constituents. The former provided closed-form formulae, but not for empty or rigid fibers, in a complicated notation, whereas the latter two did not get any final closed-form formulae for the effective properties. In fact it is possible to get the same formulae which is given in this paper through the two slightly different routes of Pobedrya (1984), which was used in Rodríguez-Ramos et al. (2001), and the other two. This is not explicitly given here.

Parton and Kudryavtsev (1993) did not produce any numerical results and share with Meguid and Kalamkarov (1994) a "misprint", which is carried out in latter equations. It says "G_M/G_F" where it should say "G_F/G_M" in Eqs. (35) and (9.21), respectively. In fact several plots in Meguid and Kalamkarov (1994) are incorrect. Here the correct ones are given. Comparison with experimental data, known bounds are other solutions (Aboudi, 1991; Luciano and Barbero, 1994; Pobedrya, 1984) is done with the exact solution. It turns out that, in a certain interval of the fiber volume fraction, some bound and the exact solution are very close to each other thus providing a simple formula, the bound, for its use in the calculation of the problem involved and giving a greater certainty in the result. See, for instance, Talbot (1999). Also closed-form expressions are given for the two microstructural parameters of Avellaneda and Swart (1998).

Section 2 starts with the statement of the problem, introducing the overall stiffnesses and engineering constants of the composite. Section 3 has the exact closed-form formulae for the overall properties of the binary composite with isotropic constituents and square symmetry. Similar formulae are also provided for two important limiting cases: of empty and rigid fibers. Various examples are considered in Section 4, where comparison among the exact solution, known bounds (Hashin, Hill and Bruno), other solutions and experimental data is discussed. Section 5 has some final remarks. The paper ends with two appendices. Appendix A defines parameters which appear in the exact formulae. Appendix B defines vectors, matrices and series relevant to the formulae.

2. Statement of the problem

A binary periodic composite is considered here in which aligned cylindrical fibers are embedded in matrix material. The direction of the fibers, which have a circular cross-section, are parallel to the Ox_3 axis. See Fig. 1. Both components have isotropic elastic properties. The periodic cell S of the composite is a square, that is, the fibers are periodically distributed without overlapping along the directions parallel to the Ox_1 and Ox_2 axes. The effective properties of this composite are tetragonal. The non-vanishing components

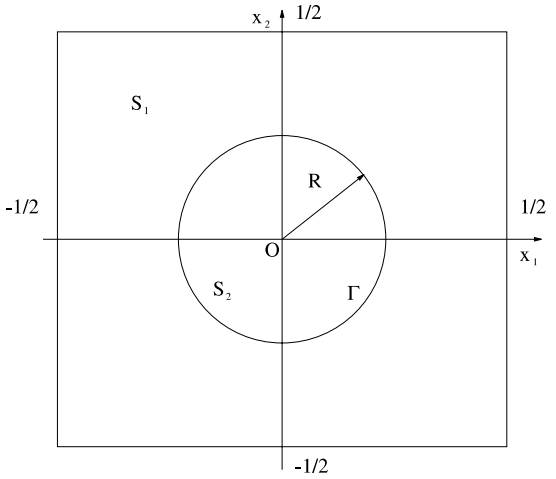

Fig. 1. It shows a cross-section of the unit square cell S of the composite, which is repeated in the directions of the Ox_1 and Ox_2 axes. The fiber occupies a circular region S_2 of radius R and center O, the matrix occupies S_1 so that $S = S_1 \cup S_2$. The common interface is Γ.

of the stress–strain relationship may be written in terms of six independent constants $\bar{k}$, $\bar{l}$, $\bar{n}$, $\bar{p}$, $\bar{m}$ and $\bar{m}'$ as follows:

$$\begin{aligned}
\tfrac{1}{2}(\bar{\sigma}_{11}+\bar{\sigma}_{22}) &= \bar{k}(\bar{\epsilon}_{11}+\bar{\epsilon}_{22})+\bar{l}\bar{\epsilon}_{33},\\
\bar{\sigma}_{33} &= \bar{l}(\bar{\epsilon}_{11}+\bar{\epsilon}_{22})+\bar{n}\bar{\epsilon}_{33},\\
\bar{\sigma}_{11}-\bar{\sigma}_{22} &= 2\bar{m}'(\bar{\epsilon}_{11}-\bar{\epsilon}_{22}),\\
\bar{\sigma}_{32} &= 2\bar{p}\bar{\epsilon}_{32},\\
\bar{\sigma}_{31} &= 2\bar{p}\bar{\epsilon}_{31},\\
\bar{\sigma}_{12} &= 2\bar{m}\bar{\epsilon}_{12},
\end{aligned} \tag{2.1}$$

where $\bar{\sigma}_{ij}$ are the components of the stress tensor, the indices i, j run from 1 to 3; the components of the strain tensor are

$$\bar{\epsilon}_{ij} = \frac{1}{2}\left(\frac{\partial \bar{u}_i}{\partial x_j}+\frac{\partial \bar{u}_j}{\partial x_i}\right), \tag{2.2}$$

here $\bar{u}_i$ are the components of the displacement vector; $\bar{k}$ is the plane-strain bulk modulus for lateral dilatation without longitudinal extension; $\bar{l}$ is the associated cross-modulus; $\bar{n}$ is the modulus for longitudinal uniaxial straining; $\bar{p}$ is the rigidity modulus for shearing in the longitudinal direction; $\bar{m}$ is the rigidity modulus for shearing in any transverse direction. In terms of these parameters, the axial, with subindex a, Young's modulus and Poisson's ratio are $\bar{E}_{\mathrm{a}}$ and $\bar{\nu}_{\mathrm{a}}$, in that order; the transverse, with subindex t, Young's modulus and Poisson's ratio, $\bar{E}_{\mathrm{t}}$ and $\bar{\nu}_{\mathrm{t}}$, respectively, are related as follows

$$\begin{aligned}
\bar{E}_{\mathrm{a}} &= \bar{n}-\bar{l}^2/\bar{k} = \bar{n}-4\bar{k}\bar{\nu}_{\mathrm{a}}^2,\\
\bar{\nu}_{\mathrm{a}} &= \bar{l}/2\bar{k},\\
\bar{E}_{\mathrm{t}} &= 4\bar{k}\bar{p}(\bar{k}+\bar{n}\bar{p}/\bar{E}_{\mathrm{a}}) = 2(\bar{l}+\bar{\nu}_{\mathrm{t}})\bar{p},\\
\bar{\nu}_{\mathrm{t}} &= (\bar{k}-\bar{n}\bar{p}/\bar{E}_{\mathrm{a}})/(\bar{k}+\bar{n}\bar{p}/\bar{E}_{\mathrm{a}}).
\end{aligned} \tag{2.3}$$

The bulk and rigidity moduli of the matrix and the fiber are denoted by K_1, μ_1, and K_2, μ_2, respectively. The area fractions occupied by the matrix and the fiber in the x_1x_2-plane are V_1 and V_2, in that order, so that

$V_1 + V_2 = 1$. Note that the percolation limit is $V_2 = \pi/4$, when the fibers are in contact. The arithmetic or Voigt average of the above properties is written by

$$\begin{aligned} K_{\mathrm{v}} &= K_1 V_1 + K_2 V_2, \\ \mu_{\mathrm{v}} &= \mu_1 V_1 + \mu_2 V_2, \end{aligned} \tag{2.4}$$

in that order.

Furthermore, the contrast of the properties K and μ across the interface Γ is written using the double bar notation, viz.,

$$\begin{aligned} ||K|| &= K_1 - K_2, \\ ||\mu|| &= \mu_1 - \mu_2, \end{aligned} \tag{2.5}$$

respectively.

The main objective of this paper is to give useful closed-form formulae for the calculation of the effective properties and its associated engineering moduli.

3. Closed-form formulae

3.1. Two-phase elastic composite

Recently, Rodríguez-Ramos et al. (2001) studied a similar fiber-reinforced composite with the same geometry except that both elastic media considered had transversely isotropic properties. The effective properties of the composite were obtained using the method of asymptotic homogeneization, and properties of doubly periodic functions. Those results can be specialized to the case of isotropic components to yield the following simple expressions:

$$\begin{aligned} \bar{k} &= K_{\mathrm{v}} + \tfrac{1}{3}\mu_{\mathrm{v}} - V_2||K + \tfrac{1}{3}\mu||^2 K_i/\mu_1, \\ \bar{l} &= K_{\mathrm{v}} - \tfrac{2}{3}\mu_{\mathrm{v}} - V_2||K + \tfrac{1}{3}\mu||||K - \tfrac{2}{3}\mu||K_i/\mu_1, \\ \bar{n} &= K_{\mathrm{v}} + \tfrac{4}{3}\mu_{\mathrm{v}} - V_2||K - \tfrac{2}{3}\mu||^2 K_i/\mu_1, \\ \bar{p} &= \mu_1[1 - 2V_2||\mu||P_i/(\mu_1 + \mu_2)], \\ \bar{m} &= \mu_1 - V_2||\mu||M_i, \\ \bar{m}' &= \mu_1 - V_2||\mu||M_i', \end{aligned} \tag{3.1}$$

where

$$\begin{aligned} K_i &= D_i[V_1 + (1+\kappa_1)D_i \mathscr{V}_p^{\mathrm{T}} \mathscr{M}_k^{-1} \tilde{\mathscr{V}}_p]/B_i, \\ P_i &= [1 + \chi \mathscr{V}_2 - \chi^2 \mathscr{V}_p^{\mathrm{T}} \mathscr{M}_p^{-1} \tilde{\mathscr{V}}_p]^{-1}, \\ M_i &= (1+\kappa_1)E_i/[1 + R^2 H_i^- - \mathscr{V}_m^{\mathrm{T}} \mathscr{M}_m^{-1} \tilde{\mathscr{V}}_m], \\ M_i' &= (1+\kappa_1)E_i/[1 + R^2 H_i^+ - \mathscr{V}_{m'}^{\mathrm{T}} \mathscr{M}_{m'}^{-1} \tilde{\mathscr{V}}_{m'}], \end{aligned} \tag{3.2}$$

where the parameters A_i, B_i, C_i, D_i, E_i, F_i, G_i, χ_μ, κ_j $(j = 1, 2)$ and χ are defined in the Appendix A, whereas the infinite order vectors $\mathscr{V}_p$, $\tilde{\mathscr{V}}_p$, $\mathscr{V}_m$, $\tilde{\mathscr{V}}_m$, $\mathscr{V}_{m'}$, $\tilde{\mathscr{V}}_{m'}$ and matrices $\mathscr{M}_k$, $\mathscr{M}_p$, $\mathscr{M}_m$, $\mathscr{M}_{m'}$ are given in Appendix B, together with $H_i^{\pm}$. The superindex T denotes a transpose vector.

It is worthwhile to see that the effective properties $\bar{k}$, $\bar{l}$, $\bar{n}$, $\bar{p}$, $\bar{m}$, and $\bar{m}'$ in Eq. (3.1) are given in terms of the properties of the two constituents, the area fraction occupied by them, the radius R of the circular cross-section and series related to doubly periodic functions of square symmetry. The four expressions K_i, M_i, P_i,

and M_i' that appear in Eq. (3.1–2) are, in fact, relatively easy to compute. Numerical experiments show that enough accurate results are obtained, when the infinite order vectors and matrices involved are truncated to the second order, because powers of R, a number less of equal than 0.5, are present and the series that appear converge very quickly. It is also interesting to mention that K_i and M_i' are related to two microstructural parameters A_k and $A_{m'}$, introduced by Avellaneda and Swart (1998). They have a simple physical interpretation, i.e., A_k and $A_{m'}$ represent, respectively, the mean transverse hydrostatic strain and mean deviatoric strain in the fiber phase, per unit applied transverse pressure and shear. Therefore,

$$\begin{aligned} A_k &= 1 + ||K - \tfrac{1}{3}\mu||K_i/\mu_1, \\ A_{m'} &= M_i'. \end{aligned} \tag{3.3}$$

Thus, Eq. (3.3) provides a closed form expression for Avellaneda and Swart (1998) microstructural parameters.

Another interesting result follows from the elimination of K_i in the first three terms of Eq. (3.1), that is to say,

$$\frac{||K + \frac{1}{3}\mu||}{||K - \frac{2}{3}\mu||} = \frac{\bar{k} - K_v - \frac{1}{3}\mu_v}{\bar{l} - K_v + \frac{2}{3}\mu_v} = \frac{\bar{l} - K_v + \frac{2}{3}\mu_v}{\bar{n} - K_v - \frac{4}{3}\mu_v}, \tag{3.4}$$

the universal relations of Hill (1964) are easily found from the exact formulae.

3.2. Empty fibers

Appropriate closed-form formulae can also be obtained for the case when the fiber is empty. The limit, when the properties of the fiber material tends to zero, yield the following closed-form expressions

$$\begin{aligned} \bar{k}_e &= (K_1 + \tfrac{1}{3}\mu_1)V_1 + (K_1 + \tfrac{1}{3}\mu_1)^2 K_e/\mu_1, \\ \bar{l}_e &= (K_1 - \tfrac{2}{3}\mu_1)V_1 - V_2(K_1 + \tfrac{2}{3}\mu_1)(K_1 - \tfrac{2}{3}\mu_1)K_e/\mu_1, \\ \bar{n}_e &= (K_1 + \tfrac{4}{3}\mu_1)V_1 - V_2(K_1 - \tfrac{2}{3}\mu_1)^2 K_e/\mu_1, \\ \bar{p}_e &= \mu_1(1 - 2V_2P_e), \\ \bar{m}_e &= \mu_1(1 - V_2M_e), \\ \bar{m}_e' &= \mu_1(1 - V_2M_e'), \end{aligned} \tag{3.5}$$

where K_e, M_e, P_e and M_e are given by Eq. (3.2) upon the substitution there of the values of the parameters A_i, B_i, C_i, D_i, G_i, E_i, χ and κ_1', as follows:

$$\begin{aligned} -A_i &= B_i = E_i = \chi = 1, \\ C_i &= -2D_i = -1/G_i, \\ \kappa_1 &= (K_1 + \tfrac{7}{3}\mu_1)/(K_1 + \tfrac{1}{3}\mu_1). \end{aligned} \tag{3.6}$$

Again the universal relations (3.4) follow with $K_2 = \mu_2 = 0$, or by the elimination of K_e from the first three terms of Eq. (3.5).

3.3. Rigid fibers

Closed-form expressions for the overall properties of rigid fibers can also be derived from Eq. (3.2) in the limit of very large values of the fiber properties. The relevant quantities become

$$\begin{aligned}
\bar{k}_r &= (K_1 + \tfrac{1}{3}\mu_1)(1 + V_2 K_r),\\
\bar{p}_r &= \mu_1(1 + 2V_2 P_r),\\
\bar{m}_r &= \mu_1(1 + V_2 M_r),\\
\bar{m}'_r &= \mu_1(1 + V_2 M'_r),
\end{aligned} \tag{3.7}$$

where

$$\begin{aligned}
K_r &= 1 + (\kappa_1 - 1)[G_i - (1 + \kappa_1)B_i \mathscr{V}_p^{\mathrm{T}} \mathscr{M}_k^{-1} \tilde{\mathscr{V}}_p / V_1]/V_1,\\
P_r &= [1 - V_2 - \mathscr{V}_p^{\mathrm{T}} \mathscr{M}_p^{-1} \tilde{\mathscr{V}}_p]^{-1},\\
M_r &= (1 + 1/\kappa_1)/[1 + R^2 H_i^- - \mathscr{V}_m^{\mathrm{T}} \mathscr{M}_m^{-1} \tilde{\mathscr{V}}_m],\\
M'_r &= (1 + 1/\kappa_1)/[1 + R^2 H_i^+ - \mathscr{V}_{m'}^{\mathrm{T}} \mathscr{M}_{m'}^{-1} \tilde{\mathscr{V}}_{m'}];
\end{aligned} \tag{3.8}$$

here, and in the infinite order vectors and matrices

$$\begin{aligned}
A_i &= \chi = -1,\\
B_i &= -1/\kappa_1 = -(K_1 + \tfrac{7}{3}\mu_1)/(K_1 + \tfrac{1}{3}\mu_1),\\
C_i &= -2\mu_1/V_1(K_1 + \tfrac{7}{3}\mu_1),
\end{aligned} \tag{3.9}$$

G_i is given by Eq. (A.1) and $H_i^{\pm}$ by Eq. (B.4).

It is interesting to note that a relation exists between P_e and P_r, namely,

$$P_e^{-1} - P_r^{-1} = 2V_2, \tag{3.10}$$

since P_e and P_r are independent of the parameter properties and depend on the square symmetry and the radius R of the fiber only.

4. Numerical examples

4.1. Two-phase elastic composite

As a first example, the same materials that were considered by Meguid and Kalamkarov (1994), Luciano and Barbero (1994), is dealt with. Here the properties are taken from Tsai and Hahn (1980) for the epoxy matrix, Young's modulus is $E_1 = 3.45$ GPa and Poisson's ratio is $\nu_1 = 0.35$, whereas the corresponding values for the glass fibers are $E_2 = 73.1$ GPa and $\nu_2 = 0.22$. It is believed that these values are representative of those used by Meguid and Kalamkarov (1994). They did not give these explicitly.

As a function of the fiber volume fraction V_2, up to the percolation limit of $\pi/4$, dimensionless plots of the effective transverse Young's modulus $\bar{E}_{\mathrm{t}}/E_1$, transverse and axial shear moduli $\bar{m}/\mu_1$, $\bar{p}/\mu_1$, axial and transverse Poisson's ratio $\bar{\nu}_{\mathrm{a}}/\nu_1$, $\bar{\nu}_{\mathrm{t}}/\nu_1$ computed using the exact formulae (continous line) are shown in Figs. 2–6, respectively. Also, in those figures, two other curves are displayed, viz., upper (dash–dotted line) and lower (dotted line) bounds. (The bounds of Hashin (1965) and Hill (1964) (see, also Christensen, 1991) for a transversely isotropic medium appear in Figs. 2, 3, 5 and 6. In Fig. 4, however, those of Bruno (1991) are plotted). Fig. 3 also shows the dimensionless modulus m'/μ_1.

It is found that the exact solution and the bounds coincide for the dimensionless axial Young's modulus $\bar{E}_{\mathrm{a}}/E_1$, like in Meguid and Kalamkarov (1994), showing an almost linear behavior. This figure is not shown

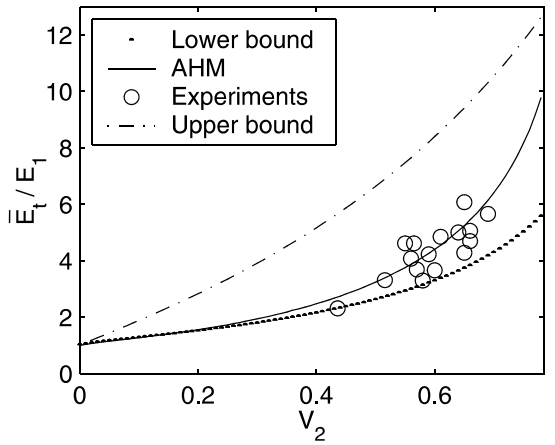

Fig. 2. Plot of the dimensionless overall transverse Young's modulus $\bar{E}_t/E_1$ against the fiber volume fraction V_2. The continuous line is computed using the exact formulae, the dash-dotted (dotted) line shows the upper (lower) bounds of Hashin (1965) and Hill (1964). Tsai and Hahn (1980) experimental data are shown as open circles.

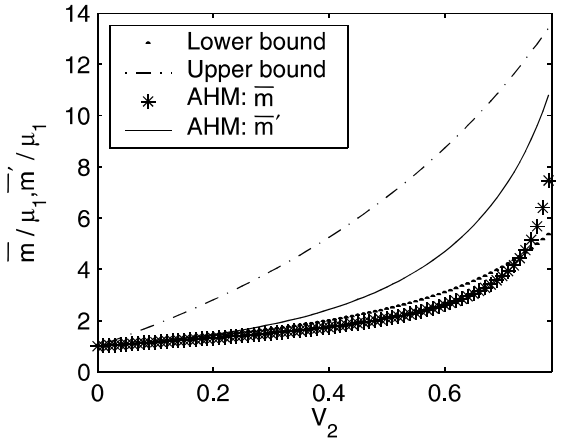

Fig. 3. Normalized transverse shear modulus $\bar{m}/\mu_1$ (star) and m'/μ_1 (continuous line) against fibre volume fraction V_2 plot, with the same conventions of Fig. 2. Note that the exact solution for $\bar{m}/\mu_1$ need not be between the bounds.

for brevity. However, the other four parameters in Figs. 2–5 show quite a different behavior from those calculated by them. The corrected ones are presented here.

The effective transverse Young's modulus $\bar{E}_t/E_1$, which lies between the bounds, increases monotonically and is closer to the lower bound up to 0.2 of the fibre volume fraction and then it deviates appreciable up to $V_2 = \pi/4$, as it can be seen in Fig. 2. The experimental data, taken from Tsai and Hahn (1980), are also shown as the open circles. The agreement is quite good between the experimental values and the exact solution, which follows the data through the middle of the data cloud. These results can also be compared with those obtained by Aboudi (1991) using the method of cells and those calculated by Luciano and Barbero (1994), who used a Fourier series technique by considering a piecewise constant eigenstrain. All the three curves show the same trend. The latter two curves are not plotted. Their behavior can easily

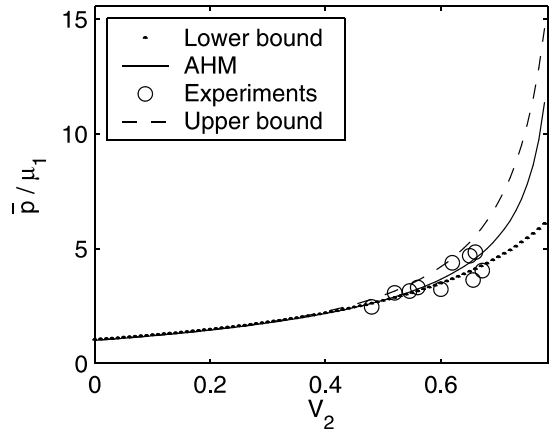

Fig. 4. Dimensionless axial shear modulus $\bar{p}/\mu_1$ versus fibre volume fraction V_2 plot. Same convention as in Fig. 2, but here the bounds are those of Bruno. The exact solution lies between the tight bonds.

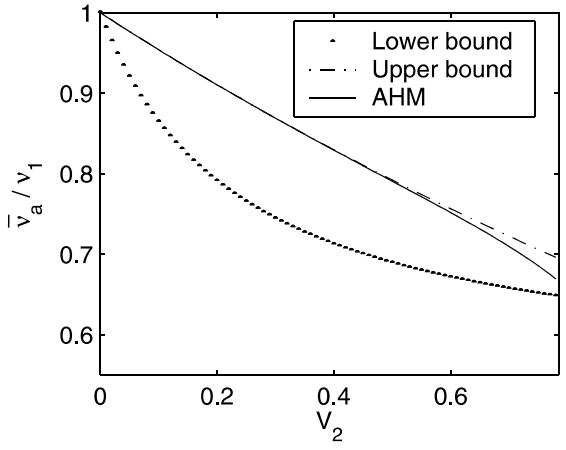

Fig. 5. Plot of the normalized axial Poisson's ratio $\bar{\nu}_a/\nu_1$ against fibre volume fraction V_2. Same conventions as in Fig. 2.

be established in relation with the data. Both curves, viz., Aboudi, Luciano and Barbero, lie next to the lower edge of the data cloud and they are close to each other. Aboudi's curve is closer to the exact solution.

As it is shown (star) in Fig. 3, the effective transverse shear modulus $\bar{m}/\mu_1$, also increases monotonically as a function of fibre volume fraction V_2 and is quite close to the lower bound except near the percolation limit. It must be recalled that the bounds plotted correspond to a transversely isotropic medium which has a different anisotropy from the tetragonal effective medium considered here. There is no reason for the exact solution to lie between these bounds. Luciano and Barbero's also computed this parameter. Their curve is an underestimate for the exact curve. A plot of m'/μ_1 against fibre volume fraction V_2 is also shown in Fig. 3. The exact solution displays a monotonically increasing value as a function of V_2, close to the lower bound up to $V_2 = 0.2$; it always lies between the two bounds.

As for $\bar{p}/\mu_1$, shown in Fig. 4, the closed-form solution increases monotonically and is closer to the lower bound up to $V_2 = 0.5$, where it deviates up to the percolation limit; it always lies between the bounds. The

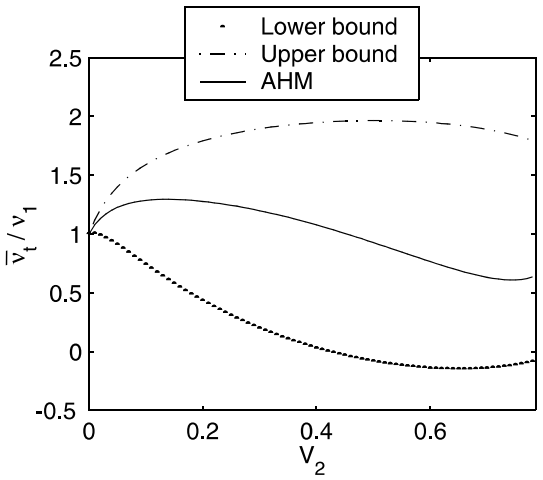

Fig. 6. Plot of the normalized transverse Poisson's ratio $\bar{v}_t/v_1$ against V_2. Same conventions as in Fig. 2.

tighter upper bound of Bruno (1991) is also shown in Fig. 4 as the dashed line. The lower bound of Bruno is the same as the Hashin–Hill lower bound. Note that the exact solution is very close to the upper bound of Bruno up to $V_2 = 0.3$ where it starts to deviate up to $V_2 = \pi/4$. This behavior is not shown by Meguid and Kalamkarov (1994) in their Fig. 3(a), where their calculated value, which is clearly wrong, lies closer to the upper Hashin–Hill bound value. Fig. 4 also shows experimental data as open circles from Tsai and Hahn (1980). The agreement of these with the exact solution is quite good, since it goes through the middle of the data cloud. The curves obtained by Aboudi (1991) and Luciano and Barbero (1994), not plotted here, show the same characteristics that were discussed for them in the Fig. 2.

In Fig. 5, the exact expression of $\bar{v}_a/v_1$, which decreases monotonically, is very similar to Luciano and Barbero's curve except near the percolation limit, which lies close to the upper bound up to $V_2 = 0.5$, where it deviates; it always lies between the bounds.

An independent check of the correctness of the calculated values using the exact formulae of this paper and tabulated values of Pobedrya (1984) was carried out. He derived formulae for the effective properties of a fiber-reinforced composite with only isotropic elastic constituents using the asymptotic homogenization method. For the ratio $\mu_2/\mu_1 = 20$, which is close to the value of 23.45 that corresponds to the materials used in the example of Figs. 2–6, the calculated normalized values here and in Pobedrya's table, have a relative error less than 0.5% except near the percolation value, where the error is larger: less than 3%. For the other values in the table, as a function of μ_2/μ_1 and V_2, the relative error is less that 3% except near the percolation limit and the larger values of μ_2/μ_1. It must be mentioned than the rigid limit has to be taken carefully. Here explicit exact formulae are also given.

The plot of the dimensionless plane Poisson's ratio $\bar{v}_t/v$ versus V_2 in Fig. 6 shows that the exact solution lies in between the Hashin bounds, not being close to any of them. It differs from the one calculated by Luciano and Barbero, specially near the percolation limit, in their case, it never is smaller than one as it is the case here beyond approximately $V_2 = 0.45$. It is interesting to note two different regimes relative to the matrix value.

Except for the latter parameter, the other properties in Figs. 2–5 show a linear behavior for small values of V_2 and then a rapid monotone one, this is consistent with the concept of a fibre-reinforced material, that is to say, the composite becomes stiffer as the (stiffer) fiber material increases, with the indicated behavior relative to V_2.

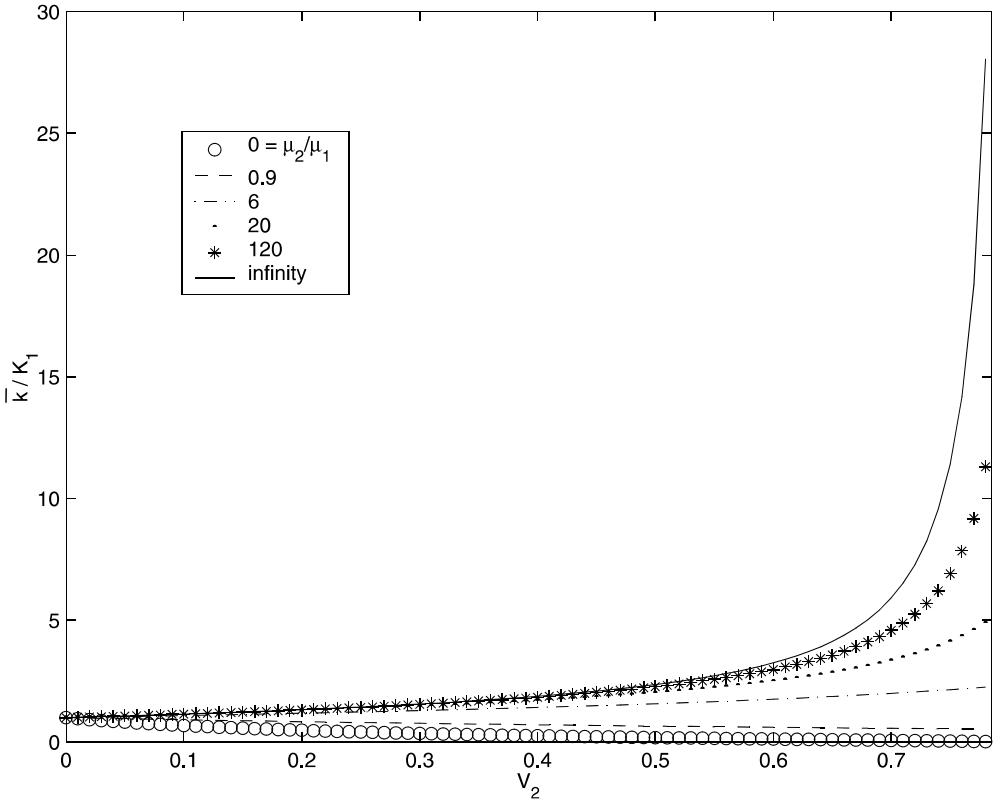

Fig. 7. Normalized overall plane bulk modulus $\bar{k}/K_1$ versus fiber volume fraction V_2 plot as a function of $z = \mu_2/\mu_1$. The shown curves are for $z = 0$ (empty fibers as open circles), 0.9 (dash), 6 (dash-dot), 20 (dots), 120 (star) and ∞ (rigid fibers as the continuous line).

It is interesting to show the dependence of the overall stiffnesses plotted versus fiber volume fraction V_2 as a function of the shear modulus ratio of the constituents materials $z = \mu_2/\mu_1$. Fig. 7 shows a plot of $\bar{k}/K_1$, versus V_2 for $z = 0$ (empty fibers as open circles), 0.9 (dash), 6 (dash-dot), 20 (dot), 120 (star) and ∞ (rigid fibers as the continuous line). There is no overlap between the curves which either increase (for $z = 6, 20, 120$ and ∞) or decrease (for $z = 0$ and 0.9) monotonically from the matrix value at zero fiber volume fraction to the percolation limit. The curves for $\bar{p}/\mu_1$, $\bar{m}/\mu_1$ and $\bar{m}'/\mu_1$ have a similar behavior as in Fig. 7, although these are not shown here for brevity. As a function of z each curve shows a linear behavior for small values of V_2 and then a rapid monotone change, either stiffer or weaker according to $z > 1$ or $z < 1$.

The exact solution for $\bar{p}/\mu_1$ is plotted as the continuous line as a function of $z = \mu_2/\mu_1$ in the range between 0 and 1 in Fig. 8; In the figure $V_2 = \pi/4$ is the percolation limit. The upper (dash-dot) and lower (dot) bounds of Bruno (1991) are also shown. In the interval [0,1], Bruno's lower bound is quite close to the exact solution and, from about $z = 0.5$ the three curves almost overlap in an almost linear fashion.

4.2. Empty fibers

The next two figures, Figs. 9 and 10 show plots against the volume fraction V_2 of three normalized axial and transverse effective parameters, respectively. The continuous line corresponds to Young's moduli, the dotted line to shear modulus and the dash-dotted line to Poisson's ratio, in the same order, in Figs. 9 and

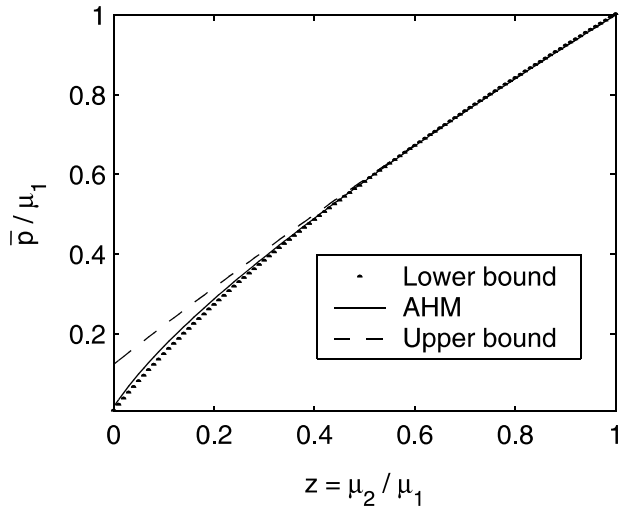

Fig. 8. Plot of normalized overall shear modulus $\bar{p}/\mu_1$ against $z = \mu_2/\mu_1$ from 0 to 1. The upper (dash-dot) and lower (dot) bounds of Bruno (1991) are also shown.

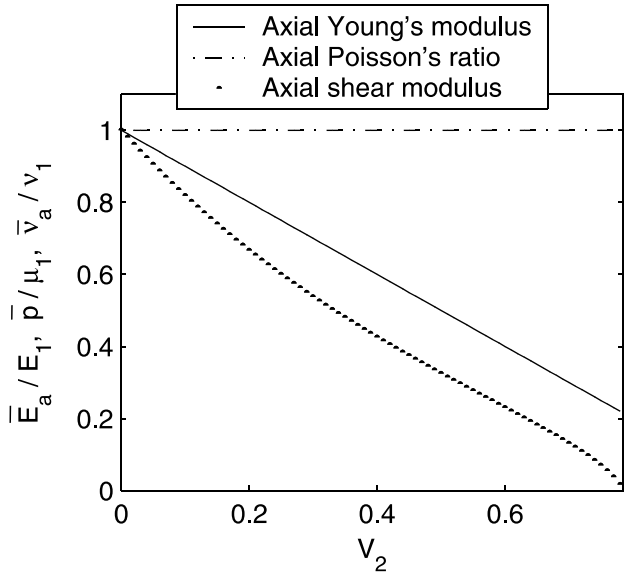

Fig. 9. Axial overall properties for empty fibers against fiber volume fraction V_2. Young's modulus $\bar{E}_a/E_1$, the continuous line; shear modulus $\bar{p}_a/\mu_1$, the dotted line; Poisson's ratio $\bar{\nu}_a/\nu_1$, the dash-dotted line.

10. The axial Poisson's ratio is constant in the whole interval. The other five parameters decrease monotonically from the matrix value. The shear modulus decreases to a near zero value at the percolation limit. The other three parameters decrease to a small value, however. It is worthwhile to note that the transverse Poisson's ratio reaches a minimum value near the percolation value and this was not shown by Meguid and Kalamkarov (1994) in their Fig. 5. In this weakened composite the moduli exhibit the diminishing effect of lesser material.

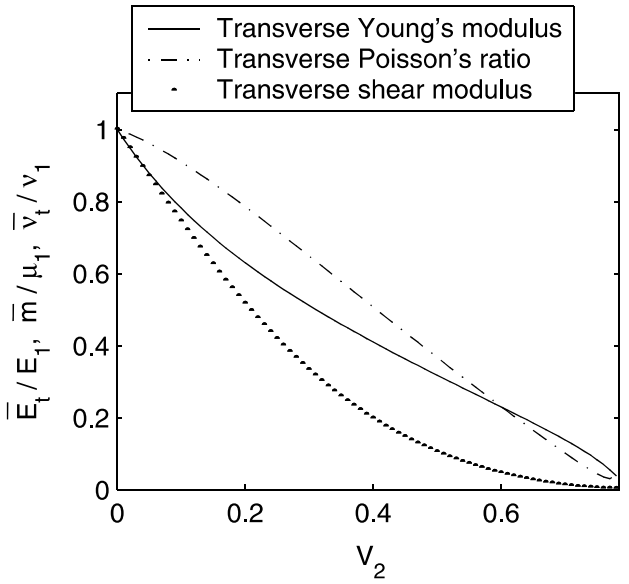

Fig. 10. Transverse effective properties for empty fibers versus fiber volume fraction V_2. Young's modulus $\bar{E}_t/E_1$, the continuous line; shear modulus $\bar{m}/\mu_1$, the dotted line; Poisson's ratio $\bar{\nu}_2/\nu_1$, the dash-dotted line.

4.3. Rigid fibers

Fig. 11 displays two plots of dimensionless axial Young's modulus $\bar{E}_a/E_1$ (continuous line) and Poisson's ratio $\bar{\nu}_t/\nu_1$ (dash-dotted line) against fiber volume fraction V_2 for rigid fibers. The Young's modulus increases monotonically from the matrix value; near the percolation limit, the increase is very rapid producing a stiffer composite. On the other hand, Poisson's ratio decreases almost linearly from the matrix value to nearly zero at $V_2 = \pi/4$.

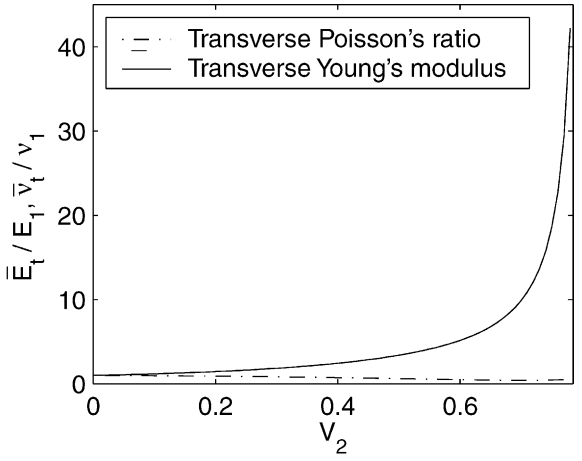

Fig. 11. Axial overall properties for rigid fibers against fiber volume fraction V_2. Young's modulus $\bar{E}_a/E_1$, the continuous line; Poisson's ratio $\bar{\nu}_t/\nu_1$, the dash-dotted line.

5. Concluding remarks

Exact closed-form formulae are given for a two-phase periodic fiber-reinforced composite, whose constituents are elastic isotropic media. The composite periodicity is square, so that the overall properties are tetragonal. Two limiting cases are considered as well, that of empty and rigid fibers for which new formulae are also given. The formulae are amenable for relatively easy computation. The series involved converge rather quickly. Not more that the second order of the infinite order vector and matrices are needed, because high powers of the radius of the circle $R \leqslant 0.5$ are present.

The results presented include comparisons with known bounds: Hashin and Hill's for transversely isotropic composite and Bruno's (1991) for dielectric material composite. In a large number of cases, the exact solution is very close to the bound in a certain interval of the fiber volume fraction V_2 or in the ratio of fiber to matrix parameters. This kind of information may be useful where the use of the simple expression given by the bound can yield easily amenable results in a certain problem. For instance, see Talbot (1999), where Bruno's bounds can produce improved bounds for a nonlinear composite.

Some of the results presented here are corrections to the ones given in Meguid and Kalamkarov (1994). A misprint in their formulae is found. It says "G_M/G_F" where it ought to say "G_F/G_M" in their Eq. (35). A full check of their equations was not done. Incidentally, the same "misprint" appears in the book of Parton and Kudryavtsev (1993) in their Eq. (9.21), etc. and possible others, which were left unchecked, because it is beyond the scope of this paper.

The comparison of the exact solution with experimental data is also very good, even better than the curves produced using other methods (Aboudi, 1991; Luciano and Bisegna, 1994). These two methods produce curves which generally lie below the one for the exact solution, and lie close to the lower edge of the set of experimental data.

Acknowledgements

This work was sponsored by CoNaCyT Project Numbers 32237-E, 27520-A, DGAPA-UNAM under grant IN 114999 and Project High Education Ministry of Cuba no. 03.50, 1999. One of the authors (FJS) would like to thank the John Simon Guggenheim Memorial Foundation for the award of one of its Fellowships. Thanks are due to Miss Ana Pérez Arteaga for computing support. The authors are also grateful to David R.S. Talbot for useful discussions and suggestions.

Appendix A

Definition of parameters that appear in some equations of Appendix B and in Eqs. (3.1) and (3.2)

$$
\begin{aligned}
A_i &= (\kappa_1\chi_\mu - \kappa_2)B_i/(\kappa_2 + \chi_\mu),\\
B_i &= (1 - \chi_\mu)/(1 + \kappa_1\chi_\mu),\\
C_i &= [(\kappa_1 - 1)\chi_\mu - (\kappa_2 - 1)]B_i/F_i,\\
D_i &= (\kappa_2 - 1)B_i/2F_i,\\
E_i &= B_i/(1 - \chi_\mu),\\
F_i &= V_1\chi_\mu + (\kappa_2 - 1)G_i,\\
G_i &= 1/2 + V_2/(\kappa_1 - 1),\\
\chi_\mu &= \mu_2/\mu_1\\
\kappa_j &= (K_j + \tfrac{7}{3}\mu_j)/(K_j + \tfrac{1}{3}\mu_j), \quad j = 1, 2,\\
\chi &= \|\mu\|/(\mu_1 + \mu_2).
\end{aligned}
\tag{A.1}
$$

Appendix B

The infinite order vectors and matrices of Eq. (3.2) are given as follows. Here $t, s = 1, 2, 3, \ldots$. The vector $\mathscr{V}_p(v_s)$, matrix $\mathscr{M}_p(m_{ts})$ and vector $\tilde{\mathscr{V}}_p(\tilde{v}_t)$, have components given by

$$\begin{aligned} v_s &= R^{8s}\eta_{1\,4s-1}, \\ m_{ts} &= \delta_{4t-1\,4s-1} - \chi^2 R^{8s}\sum_{i=1}^{\infty} R^{8i}\eta_{4t-1\,4i+1}\ \eta_{4i+1\,4s-1}, \\ \tilde{v}_t &= \eta_{4t-1\,1}, \end{aligned} \tag{B.1}$$

where δ_{ts} is Kronecker's delta; it is equal to one, if $t = s$ and zero otherwise. For a definition of χ and the parameters below A_i, B_i, C_i, see Appendix A.

Similarly, for $\mathscr{V}_{m'}(v_s^+)$, $\mathscr{M}_{m'}(m_{ts}^+)$, $\tilde{\mathscr{V}}_{m'}(\tilde{v}_t^+)$ and $\mathscr{V}_m(v_s^-)$, $\mathscr{M}_m(m_{ts}^-)$, $\tilde{\mathscr{V}}_m(\tilde{v}_t^-)$, the components are defined as follows

$$\begin{aligned} v_s^{\pm} &= R^{8s+4}(\pm A_i r_{1\,4s+1} + B_i g_{1\,4s+1}), \\ m_{ts}^{\pm} &= \delta_{4t+1\,4s+1} + R^{8s+2}(A_i r_{4t+1\,4s+1} \pm B_i g_{4t+1\,4s+1}), \\ \tilde{v}_t^{\pm} &= \pm A_i r_{4t+1\,1} + B_i g_{4t+1\,1}, \end{aligned} \tag{B.2}$$

the matrix $\mathscr{M}_k(m_{ts})$ has components defined next

$$m_{ts} = \delta_{4t-1\,4s-1} + R^{8s-2}(A_i r_{4t-1\,4s-1} + B_i g_{4t-1\,4s-1} + C_i R^2 \eta_{4t-1\,1}\ \eta_{1\,4s-1}). \tag{B.3}$$

Finally,

$$H_i^{\pm} = A_i r_{11} + B_i[\pi(\kappa_1 \pm 5S_4/\pi^2) \pm g_{11}]. \tag{B.4}$$

The above formulae involve certain convergent series related to the doubly periodic elliptic functions of periods $\omega_1 = 1$ and $\omega_2 = i$ defined below

$$\begin{aligned} S_{k+l} &= {\sum_{m,n}}' \beta_{mn}^{-k-l} \qquad \text{for } k + l \geqslant 3, \\ T_{k+l} &= {\sum_{m,n}}' \bar{\beta}_{mn}\beta_{mn}^{-k-l-1} \quad \text{for } k + l \geqslant 3, \\ \eta_{kl} &= -C_{k+l-1}^{l} S_{k+l}, \\ \eta'_{kl} &= C_{k+l}^{l} T_{k+l}, \end{aligned} \tag{B.5}$$

where $\beta_{mn} = m\omega_1 + n\omega_2, m, n = 0, 1, 2, \ldots$, the prime on the sigma symbol denotes that the double summation excludes the term $m = n = 0$ and $C_k^l = k!/l!(k-l)!$ $S_2 \equiv T_2 \equiv 0$. Also,

$$\begin{aligned} r_{kl} &= \sum_{i=3}^{\infty}{}^{\mathrm{o}} R^2 \eta_{ki}\eta_{il}, \\ g_{kl} &= k\left(\frac{k+l+2}{l+1} R^2 \eta_{k+2\,l} + \eta'_{kl}\right), \end{aligned} \tag{B.6}$$

for $k, l = 1, 3, 5, \ldots$. The superindex o on the sigma symbol means that the summation is carried only over odd indices. The double series $\sum_{k,l} g_{kl}$ and $\sum_{k,l} r_{kl}$ are absolutely convergent. The above series converge very quickly.

References

Aboudi, J., 1991. Mechanics of Composite Materials. A Unified Micromechanical Approach. Elsevier, Amsterdam.
Avellaneda, M., Swart, P.J., 1998. Calculating the performance of 1–3 piezoelectric composites for hydrophone applications: an effective medium approach. J. Acoust. Soc. Am. 103, 1449–1467.
Bensoussan, A., Lions, J.L., Papanicoloau, G., 1978. Asymptotic Analysis for Periodic Structures. North-Holland, Amsterdam.
Bakhvalov, N.S., Panasenko, G.P., 1989. Homogenization Averaging Processes in Periodic Media. Kluwer, Dordrecht.
Bruno, O., 1991. The effective conductivity of strongly heterogeneous composites. Proc. R. Soc. Lond. A 443, 353–381.
Christensen, R.M., 1991. Mechanics of Composite Materials. Krieger, Malabar, FL.
Hashin, Z., 1965. On elastic behaviour of fibre reinforced materials of arbitrary transverse phase geometry. J. Mech. Phys. Solids 13, 119–134.
Hill, R., 1964. Theory of mechanical properties of fiber-strengthened materials: I. Elastic behaviour. J. Mech. Phys. Solids 12, 199–212.
Iwakuma, T., Nemat-Nasser, S., 1983. Composites with periodic microstructure. Int. J. Solids Struct. 16, 13–19.
Kalamkarov, A.L., Kolpakov, A.G., 1997. Analysis, Design and Optimization of Composite Structures. Wiley, Chichester, UK.
Lions, J., 1981. Some Methods in the Mathematical Analysis. Analysis of Systems and their Control. Gordon and Breach, New York.
Luciano, R., Barbero, E.J., 1994. Formulas for the stiffness of composites with periodic microstructure. Int. J. Solids Struct. 31, 2933–2944.
Meguid, S.A., Kalamkarov, A.L., 1994. Asymptotic homogenization of elastic composite materials with a regular structure. Int. J. Solids Struct. 31, 303–316.
Nemat-Nasser, S., Hori, M., 1999. Micromechanics: Overall Properties of Heterogeneous Materials. North-Holland, Amsterdam.
Oleinik, O.A., Shamaev, A.S., Yosifian, G.A., 1992. Mathematical Problems in Elasticity and Homogenization. North-Holland, Amsterdam.
Parton, V.Z., Kudryavtsev, B.A., 1993. Engineering Mechanics of Composite Structures. CRC Press, Boca Raton.
Pobedrya, B.E., 1984. Mechanics of Composite Materials. Moscow State University Press, Moscow (in Russian).
Rodríguez-Ramos, R., Sabina, F.J., Guinovart-Díaz, R., Bravo-Castillero, J., 2001. Closed-form expressions for the effective coefficients of a fiber-reinforced composite with transversely isotropic constituents-I. Elastic and square symmetry. Mech. Mat. 33, 223–235.
Sánchez-Palencia, E., 1980. Non homogeneous media and vibration theory. Lecture Notes in Physics, vol. 127, Springer, Berlin.
Talbot, D.R.S., 1999. Bounds which incorporate morphological information for a nonlinear composite dielectric. Proc. Roy. Soc. Lond. A 455, 3617–3628.
Tsai, S.W., Hahn, H.T., 1980. Introduction to Composite Materials. Technomic, Westport.